SELF-ALGINED SELF-DOPING SELECTIVE EMITTER FOR SCREEN-PRINTED SILICON SOLAR CELLS

A. Rohatgi[1] , M. Hilali[1], D. L. Meier[2], A. Ebong[1], C. Honsberg[1] , A. F. Carrol[3], and P. Hacke[2]
[1]University Center of Excellence for Photovoltaics Research and Education, School of Electrical and Computer Engineering, Georgia Institute of Technology, Atlanta, GA 30332-0250
[2]Ebara Solar, Inc.
13 Airport Rd., Belle Vernon, PA 15012
[3]Dupont Microcircuit Materials
14 Alexander Drive, Research Triangle Park, NC 27709

ABSTRACT: A self-aligned selective emitter for screen-printed solar cells is described in which phosphorus dopant is incorporated into a silver paste and diffused into the silicon. This produces an ohmic contact on 70-100 Ω/□ emitter due to the doping of silicon underneath the Ag grid. Alloying is performed in a belt furnace at 900°C for 2 min, above the Ag-Si eutectic temperature of 835°C. SIMS analysis showed a surface doping concentration of $1x10^{21}$ cm^{-3} for a fritless paste (Dupont PV167) and $2x10^{19}$ cm^{-3} for the fritted paste (PV 168). Sheet resistance due to self-doping alone was quite high 121 Ω/□ and 700 Ω/□ for the PV167 and PV168 pastes, respectively. Therefore, a light diffusion is required underneath the Ag to achieve good ohmic contact. Fritted paste was successfully fired through the SiN_x AR coating producing a reasonable ohmic contact to the n^+ layers doped up to 100 Ω/□ sheet resistance. PC1D model calculations revealed that a selective emitter induced performance enhancement is a function of base resistivity, front- and back-surface recombination velocities, and bulk lifetime. For example, if the front-surface recombination velocity (FSRV) is very high (>100,000 cm/s), then the selective emitter under-performs the conventional 40 Ω/□ homogeneous emitter cell. However, if the FSRV is 10000 cm/s the selective emitter gives a 0.6% (absolute) increase in cell efficiency. Selective emitter cells fabricated with 70-80 Ω/□ sheet resistance between the gridlines produced approximately 16% and 15% efficient cells on float-zone and cast multicrystalline Si materials. Series resistance of 0.75 Ω-cm^2 and a fill factor of ~0.76 were achieved. Selective emitter cells were about 0.3% (absolute) more efficient than the conventional cells with 45 Ω/□ homogeneous emitter. Cell analysis revealed that a reduced FSRV could result in greater improvement.
Keywords: Selective Emitter – 1: Self-doping Paste – 2: Screen Printing – 3

1. INTRODUCTION

Most cell manufacturers use screen-printed (SP) Ag contacts because screen-printing is a simple, rapid, and cost effective technology. However, today cost and throughput gains are obtained at the expense of the FF and cell performance. Most commercial cells have a FF of 0.75 or less compared to a FF of 0.80 or higher for the laboratory cells with photolithography contacts. Screen-printed Ag contacts generally require an emitter sheet resistance of ≤45 Ω/□ to achieve marginally acceptable contact resistance and FF [1]. In addition, such high doping in the emitter reduces the short wavelength response due to the heavy doping effects and poor FSRV. A selective emitter with heavy doping only beneath the grid can allow 70-100 Ω/□ sheet resistance between the grid. This could give good ohmic contact and FF while reducing the heavy doping effects in the emitter. Selective emitters have been previously formed by selectively printing a phosphorus diffusion paste [2, 3]. Selective emitters have also been fabricated by a self-aligned plasma-etchback technique using screen-printed gridlines as masks [4]. This paper describes the formation of a self-aligned selective emitter (heavy doping beneath the metal and light doping between the metal grid) that requires no extra processing steps. The dopant is introduced into the Si by an alloying reaction at 900°C (above the Ag-Si eutectic temperature of 835°C). This is similar to the way Al is introduced into the Si during the Al back-surface field (BSF) formation. Model calculations are performed to determine cell designs that give greater improvement due to the selective emitter and when the selective emitter is not beneficial. Finally, selective emitter cells are fabricated and analyzed on float-zone and cast multicrystalline (mc-Si) to understand and quantify the benefit of selective emitter cells.

2. MODELING THE EFFECT OF SELECTIVE EMITTER ON SCREEN PRINTED CELL PERFORMANCE

This section shows that in order for the selective emitter to be effective, certain cell design criteria must be satisfied. PC1D modeling is used to quantify the performance enhancement due to the selective emitter for various cell designs. Table I shows the PC1D -inputs for this calculation.

Figure 1 shows the efficiency improvement due to the selective emitter, relative to a conventional 40 Ω/□ homogeneous emitter cell, as a function of base resistivity. It is important to note that in these calculations the back-surface recombination velocity (BSRV) was reduced for the higher resistivity Si because of the increase in doping step height of the high-low junction. Figure 1 shows that for a 1.3 Ω-cm base resistivity, used for most current industrial cells, a selective emitter with a 110 Ω/□ sheet resistance between the gridlines gives 0.67% increase in absolute efficiency. Since PC1D is a one-dimensional model, the selective emitter was modeled with 110 Ω/□ homogeneous sheet resistance with a constant FSRV. Selective emitter and conventional cell efficiencies were 16.5% and 15.8%, respectively, for the inputs shown in Table I.

Table I: Modeling parameters for the n^+-p-p^+ solar cells.

Device Parameter		PC1D Input
Thickness		300 μm
Resistivity		1.3 Ω-cm
BSRV		1000 cm/s
FSRV	40 Ω/sq.-conventional cell	200 000 cm/s
	110 Ω/sq.-selective emitter	7000 cm/s
Series Resistance		0.6 Ω-cm^2
Shunt Resistance		3333 Ω-cm^2
J_{02}		5 nA/cm^2
n_2		2.1
Front Surface Reflectance		Single Layer ARC: t = 790 Å, n = 2.0
Grid Shadowing		5%
Texturing		None
Rear Internal Reflectance		45 % Diffuse
Lifetime (τ)		30 μs

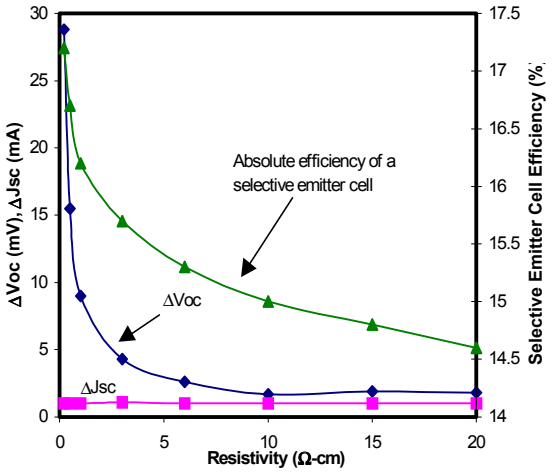

Figure 1: The absolute efficiency of a selective emitter solar cell, and the change in open-circuit voltage and short-circuit current (relative to a 40 Ω/☐ emitter cell) as a function of base resistivity.

For base resistivities less than 1 Ω-cm, the improvement in efficiency due to the selective emitter is very rapid. For resistivities between 1 Ω-cm and 10 Ω-cm there is almost a linear improvement in efficiency with the decrease in resistivity. However, for resistivities greater than 10 Ω-cm, the improvement in efficiency due to the selective emitter stays constant at 0.4% absolute.

Emitter and base leakage current densities (J_{oe} and J_{ob}) in Fig. 2 reveal that above 10 Ω-cm resistivity, J_o is dominated by J_{ob}, which is the same for both the cells. Therefore, J_o, V_{oc}, and efficiency do not change with base resistivity, and the efficiency enhancement is limited by the increase in J_{sc} due to the reduced recombination in the emitter. As we lower the base resistivity, J_{ob} decreases. Since the Joe of the 40 Ω/☐ is higher than that for the 110 Ω/☐ selective emitter, $J_o = J_{oe} + J_{ob}$ of the conventional cells becomes higher while J_o of the selective emitter cell remains ≈ J_{ob}. As a result, the efficiency enhancement due to selective emitter rises as we decrease the resistivity below 10 Ω-cm (Fig. 1). It should be noted that the bulk lifetime was maintained at 30 μs for all resistivities in these calculations.

Figure 3 shows that the front surface recombination velocity (FSRV) is very critical in realizing the full benefit of selective emitter. In these calculations bulk lifetime, BSRV, and base resistivity were fixed at 30 μs, 1,000 cm/s, 1.3 Ω-cm respectively. The FSRV of a conventional cell was fixed at 200,000 cm/s, while the FSRV for the 110 Ω/☐ selective emitter cell was varied from 10^3-10^6 cm/s.

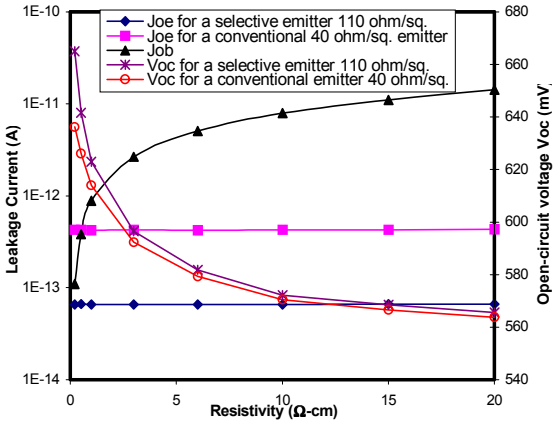

Figure 2: Plots of the leakage currents (J_{oe} and J_{ob}) and open-circuit voltage (V_{oc}) for a selective and a conventional emitter.

The data indicates that for a FSRV greater than 120,000 cm/s, the selective emitter actually under-performs the conventional cell because a transparent emitter with high FSRV lowers the V_{oc} and J_{sc}. However, if the FSRV can be lowered to 10,000 cm/s, then the selective emitter can increase the performance by 0.60% absolute. This crossover point is a function of the FSRV selected for the conventional emitter. If that value is increased from 200,000 cm/s to 500,000 cm/s then the curve becomes almost asymptotic with the FSRV axis with the crossover point approaching 10^6 cm/s.

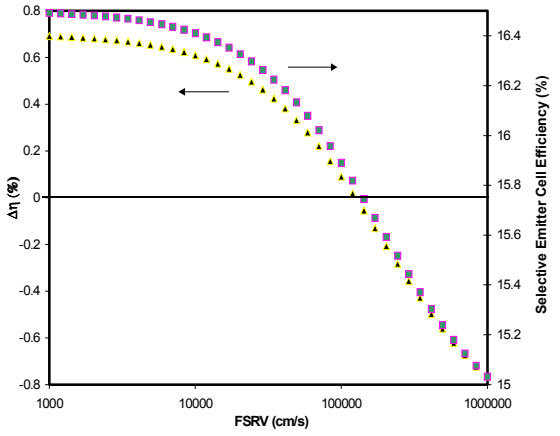

Figure 3: Improvement in efficiency of a selective emitter cell relative to the 40 Ω/☐ conventional emitter cell, and its absolute efficiency as a function of FSRV. The FSRV of the conventional emitter cell was fixed at 200,000 cm/s.

Figure 4 the improvement (compared to a conventional 40 Ω/☐ emitter cell) in efficiency due to a selective emitter for a BSRV of 600 cm/s and a 15,000 cm/s. Thus, if we reduce the base resistivity of cells from 1-2 Ω-cm to 0.7 Ω-cm, while maintaining 30 µs lifetime, lower the FSRV to 1,000 cm/s, lower the BSRV to 600 cm/s, then a selective emitter with ~110 Ω/☐ between the gridlines can improve the efficiency by 0.7%. Similar calculations for a 70Ω/☐ selective emitter gave efficiency enhancement of 0.6% over the conventional 40 Ω/☐ emitter cell with an FSRV of 200,000, bulk lifetime of 30 µs and a resistivity of 1.3 Ω-cm. If the selective emitter also improves the fill factor from 0.74 to 0.77 due to the heavy surface doping under the gridline, then, the improvement could be even higher.

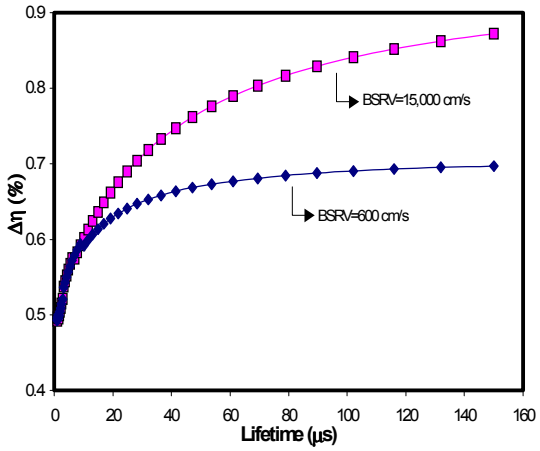

Figure 4: Improvement in efficiency (compared to a conventional 40 Ω/☐ emitter cell) due to a 110 Ω/☐ selective emitter cell for a BSRV of 600 cm/s and 15,000 cm/s.

3. DEVICE FABRICATION

Two types of screen-printed solar cells were fabricated: conventional cell with 40 Ω/☐ homogeneous emitter, and selective emitter cell with ~70-80 Ω/☐ diffusion between the metal gridlines. For conventional cells, 40 Ω/☐ diffusion was performed by a spin-on source at 935°C for 6 min in the belt furnace. PECVD single layer AR coating was deposited on the front and Al metal was screen-printed on the back followed by an 850°C/2 min anneal in the belt furnace to form an alloyed Al BSF. A silver paste from Ferro Corporation was used to screen print Ag gridlines on top of the SiN_x followed by 735°C/40 sec anneal. This punches through the SiN_x AR coating and forms ohmic contact to the emitter surface.

Selective emitter cells were formed by a 6 min spin-on doped phosphorus diffusion in a belt furnace at 925°C. This resulted in a ~75 Ω/☐ emitter with a junction depth of ~ 0.25 µm. After the phosphorus removal and DI water rinse, a single layer PECVD SiN_x antireflection coating was deposited on the front at 300°C. This was followed by Al screen printing on the back and 2 minute drive-in at 860°C in the belt furnace to form an effective back surface field. A self-doping Ag paste (Dupont PV168) was screen-printed on top of SiN_x followed by a burn-off step at 425°C and alloying at 900°C for 2 min. This method of fabricating a selective emitter does not require any extra processing steps and is self-aligned in which the dopant required beneath the silver contacts is present as an integral component of the silver-dopant system. The Ag self-doping paste introduces the dopant (phosphorus) into the silicon via an alloying reaction at a processing temperature above the silver-silicon eutectic temperature of 835°C. This is similar to forming the Al BSF.

4. RESULTS AND DISCUSSION

Two types of self-doping pastes were investigated, one with glass frit (PV168) and the other without the frit (paste PV167). Figure 5 shows the SIMS profiles for phosphorus in silicon underneath the grid after firing these Ag pastes on a bare Si (boron-doped) surface at 900°C in the belt furnace.

Fritless paste PV167 gave a much higher surface concentration than PV168, suggesting that glass frit tends to retard the incorporation of P into Si. Since our standard cell process involves firing the Ag paste through the SiN_x, we had to use PV168 for cell fabrication. Fritless paste does not punch through the SiN_x film. SIMS data (Fig. 5) showed that 900°C alloying produces a surface concentration of $\geq 2 \times 10^{19}$ cm^{-3} which drops off quite rapidly, resulting in a much higher sheet resistance (700 Ω/☐) than desired. Table II shows the calculated sheet resistance from the SIMS data for the two self-doping pastes after the belt-firing process.

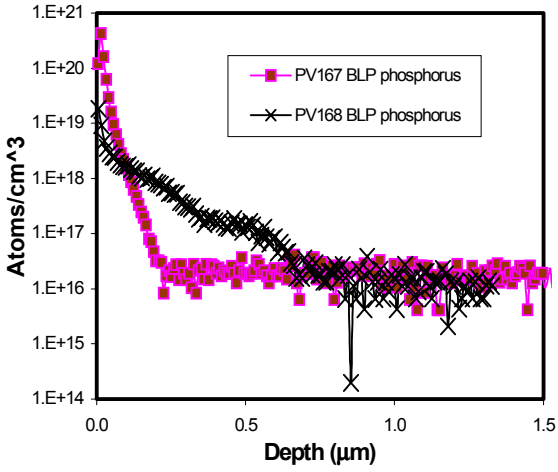

Figure 5: SIMS data for the PV168 and PV167 self-doping silver pastes showing the phosphorus concentration in silicon after 900° firing in the belt-line furnace.

We screen-printed and fired the PV168 paste on three Si substrates with base doping ranging from 10^{15}-2×10^{19} cm^{-3}. The TLM pattern was screen printed to measure the contact resistance. With uniform 2×10^{19} cm^{-3} phosphorus doping underneath the Ag paste, PV168 gave a fairly good contact resistance (~2 mΩ-cm^2). However, the contact resistance increased rapidly when the bulk doping concentration was below 10^{18} cm^{-3}. More significantly, PV168 gave unacceptable high contact resistance on undiffused Si wafers with base doping of ~10^{15} cm^{-3} because of high sheet resistance (700 Ω/☐), even though the surface concentration was 2×10^{19} cm^{-3} after 900°C/2 min alloying (Fig. 5).

Contact resistance of the Dupont PV168 Ag paste fired through the SiN_x AR coating to an underlying n^+ layer was found to be acceptably low for n^+ layers with sheet resistance values up to 100 Ω/□. The TLM method gave a contact resistance of 1-3 mΩ-cm^2 on a 75 Ω/□ diffusion, which should have a negligible effect on the series resistance, and 12 mΩ-cm^2 on a 93 Ω/□ n^+ diffusion, which should lower FF by only 0.01 for normal grid patterns [5]. Since only a light diffusion (≤100 Ω/□) is needed for good contact for the PV168 paste, it allows the formation of the selective emitter. Conventional Ag pastes do not inject enough phosphorus to help the ohmic contact formation on ≥ 70 Ω/□ emitters. Instead, the surface concentration could decrease if the frit in the paste etches even a very thin layer of Si.

Table II: Measured sheet resistance after the belt-line firing of the two self-doping pastes on 1.3 Ω-cm p-type float zone Si.

Paste	Process	Calculated Sheet Resistance from SIMS (Ω / □)
PV167	BLP 900 °C/6 min.	121
PV168	BLP 900 °C/2 min.	700

After establishing phosphorus incorporation underneath the alloyed PV168 Ag grid with a surface concentration of ≥2x10^{19} cm^{-3} and a contact resistance of 1-3 mΩ-cm^2 on a 75 Ω/□ n^+ diffused layer, we fabricated n^+-p-p^+ conventional and selective emitter cells according to the process sequence outlined in Section 3. Tables III and IV summarize the cell results from the light and dark I-V measurements. Cell ID in the tables denotes the substrate material, which includes float-zone, HEM and Bayer cast mc-Si. Selective emitter cells with 75 Ω/□ n^+ layer generally gave comparable or slightly lower series resistance and a higher FF relative to the conventional cells with a 40-45 Ω/□ emitter. Series resistance for the selective emitter cells was ~0.75 Ω-cm^2 with shunt resistance in the range of 2-25 kΩ-cm^2. Tables III and IV show that the selective emitter cells gave ≈0.3% higher efficiency compared to the counterpart conventional cells.

In order to further understand and explain the difference between the selective emitter and conventional cells, IQE measurements were performed. In the short wavelength range the selective emitter showed only a slightly higher IQE. Attempts to fit the short wavelength IQE with PC1D, using the 70 Ω/□ profile for the selective emitter gave an FSRV of ~500,000 cm/s, which is too high to realize the full benefit of the selective emitter. That is why the selective emitter induced performance enhancement was limited. Better surface passivation should increase the benefit of this selective emitter.

5. CONCLUSIONS

A self-aligned selective emitter is formed by achieving an acceptable ohmic contact to 70-100 Ω/□ by incorporating phosphorus underneath the screen-printed Ag grid. Alloying of a fritted Ag paste (Dupont PV168) at 900°C, above the Ag-Si eutectic temperature of 835°C, produces a phosphorus surface concentration of 2x10^{19} cm^{-3} and contact-resistance of 2-12 mΩ-cm^2 on 70-100 Ω/□ emitters. Model calculations reveal that the front-surface recombination velocity should be <10^4 cm/s to realize the full benefit from selective emitter cells. Selective emitter cells fabricated on float zone and cast mc-Si gave cell efficiencies of ~16% and ~15%, respectively, which were about 0.3% better than the conventional cells. Cell analysis showed that the performance enhancement due to the selective emitter was limited because of the high front-surface recombination velocity.

Table III: Cell I-V data using the self-doping paste on a surface with 70-75 Ω/□ sheet resistance.

Cell ID	V_{oc} (mV)	J_{sc} (mA/cm^2)	FF	Eff (%)	R_s (Ω-cm^2)	R_{sh} (kΩ-cm^2)
Fz1	632	33.8	0.757	16.2	0.78	9.19
HEM1	610	31.8	0.753	14.6	0.70	8.78
Bmc1	621	32.2	0.760	15.2	0.75	23.4

Table IV: Cell I-V data using the regular paste on a surface with 40-45 Ω/□ sheet resistance.

Cell ID	V_{oc} (mV)	J_{sc} (mA/cm^2)	FF	Eff (%)	R_s (Ω-cm^2)	R_{sh} (kΩ-cm^2)
Fz2	624	33.4	0.765	16	0.65	9.13
HEM2	609	31.9	0.745	14.5	0.88	83.3
Bmc2	617	32.2	0.731	14.6	0.94	0.76

ACKNOWLEDGEMENTS

The authors wish to thank Dr. Bhushan Sopori and Sally Asher of NREL for providing the SIMS measurement data. The authors would also like to thank Ajay Upadhyaya for his help in some of the experimental work. This work was supported by DOE contract No. DE-FC36-00GO10600.

REFERENCES

[1] J. Szlufcik, H. E. Elgamel, M. Ghannam, J. Nijs, R. Mertens, Appl. Phys. Lett. **59** (1991) 1583.

[2] J. Horzel, J. Szlufcik, M. Honore, J. Nijs, R. Mertens, Proceedings 14th EC Photovoltaic Solar Energy Conference, Barcelona Spain (1997) 61.

[3] J. Horzel, J. Szlufcik, J. Nijs, R. Mertens, Proceedings 26th Photovoltaic Solar Energy Conference, Anaheim CA (1997) 139.

[4] D. S. Ruby, P. Yang, M. Roy, S.Narayanan, Proceedings 26th Photovoltaic Solar Energy Conference, Anaheim CA (1997) 39.

[5] D. L. Meier, H. P. Davis, R. A. Garcia, J. A. Jessup, Proceedings 28th Photovoltaic Solar Energy Conference, Anchorage Alaska (2000) 69.